

On the improvement of buckling of pretwisted universal steel columns



Farid H. Abed ^{*}, Mai Megahed ¹, Abdulla Al-Rahmani ¹

Department of Civil Engineering, American University of Sharjah, P.O. Box 26666, Sharjah, UAE

ARTICLE INFO

Article history:

Received 1 August 2015

Received in revised form 21 October 2015

Accepted 29 October 2015

Available online 6 November 2015

Keywords:

Pretwisting
UC sections
Buckling
FE simulation
Columns

ABSTRACT

This paper investigates the improvement in elastic buckling capacity of pretwisted columns using Linear Perturbation Approach. Three different Universal Column (UC) sections of various lengths were considered in the proposed study assuming fixed–fixed and pinned–pinned end conditions. Linear perturbation analysis was first verified by comparing the critical loads of the simulated straight columns with analytical results. Numerical analysis was then extended to simulate the buckling improvement of pretwisted columns considering four different lengths of 4 m, 5 m, 6 m and 7 m, and a range of twisting angles between 0° and 180°. The results showed that the initial twisting has positively impacted the axial capacity of the pretwisted columns. This noticeable improvement is supported by the significant increase in the buckling capacity for the three UC sections, particularly at angles of twists between 120° and 150°.

© 2015 The Institution of Structural Engineers. Published by Elsevier Ltd. All rights reserved.

1. Introduction

Steel structures are increasingly used in constructions as they proved to be more user- and environmental-friendly, more time efficient and less labor intensive than reinforced concrete. Steel is a recyclable material that can be reused when a building is demolished, leaving behind minimal waste, thus, preferable for sustainable construction. Furthermore, the uniformity and stability of steel as it does not creep or shrink with time unlike reinforced concrete makes it more desirable to be used in construction. However, one of the main disadvantages of a steel column is the susceptibility to buckle under compression before achieving the design strength. Buckling is a mode of failure that is mainly observed in compression members due to structural instability. The critical buckling load carried depends mainly on the slenderness of the member being investigated. For stocky members, a larger buckling load would be required to witness the deformed buckling mode. As a matter of fact, stocky compression members may fail mainly due to compressive yielding instead of buckling. Compressive yielding may occur if the stresses built within the compression members exceeded the yielding stress of the steel being used. However, for slender members, to be more specific, the stress just before buckling is below the proportional limit such that the member is still elastic [12].

Inducing a natural pretwist along the length of a column section makes the column have a different resistance at every point along its centroidal axis. It is well-known that a column usually buckles around the weak axis, but with pretwisting, the buckling mode of the column

may no longer be perpendicular to the weak axis. Pretwisting is known to induce a coupling effect on the weak and strong flexural planes of a column. Hence, a pretwisted column in 3D-space has its strong flexural plane weakened and its weak flexural plane strengthened, leading to a net favorable effect on the buckling strength of the pretwisted column. Thus, the buckling load recorded with the first mode shape of the pretwisted column is relatively higher than that of the non-pretwisted column [15]. Another interesting definition of pretwisting would be; the rotation of the principal axes as a function of the centroidal axes of the cross-section along the column's length [3].

There are not enough studies on the topic of pretwisting and its effect on the buckling of structural compression members. However, the study of the nature of pretwisting and its applications has been introduced into the literature a long time ago. Celep [3] investigated the stability of an elastic cantilever column with a linear viscous internal damping system exposed to evenly distributed vertical and follower loads. Galerkins' technique was then applied to solve the prevailing differential equations of motion to determine the flexural deformation in both planes of a pretwisted slender column. Yang and Yau [16] studied the stability of pretwisted bars having assorted end torques. Two types of torques were investigated; quasi tangential and semi-tangential, on an originally straight bar but with an applied rotation angle. Tabarrok et al. [15] solved the equilibrium equations of buckling analysis of a pretwisted column utilizing the concept of total potential energy and the associated boundary conditions. Steinman et al. [14] studied the effect of pretwisting on statically determinate and indeterminate columns. To work out the buckling equations of a pretwisted column, the general stability equations applied for a spatial rod were used as a part of the derived differential equations. Exact numerical solutions to the controlling fourth-order differential equations were achieved through simple iterative approach. The input data to the

^{*} Corresponding author.

E-mail address: fabed@aus.edu (F.H. Abed).

¹ Master Student.

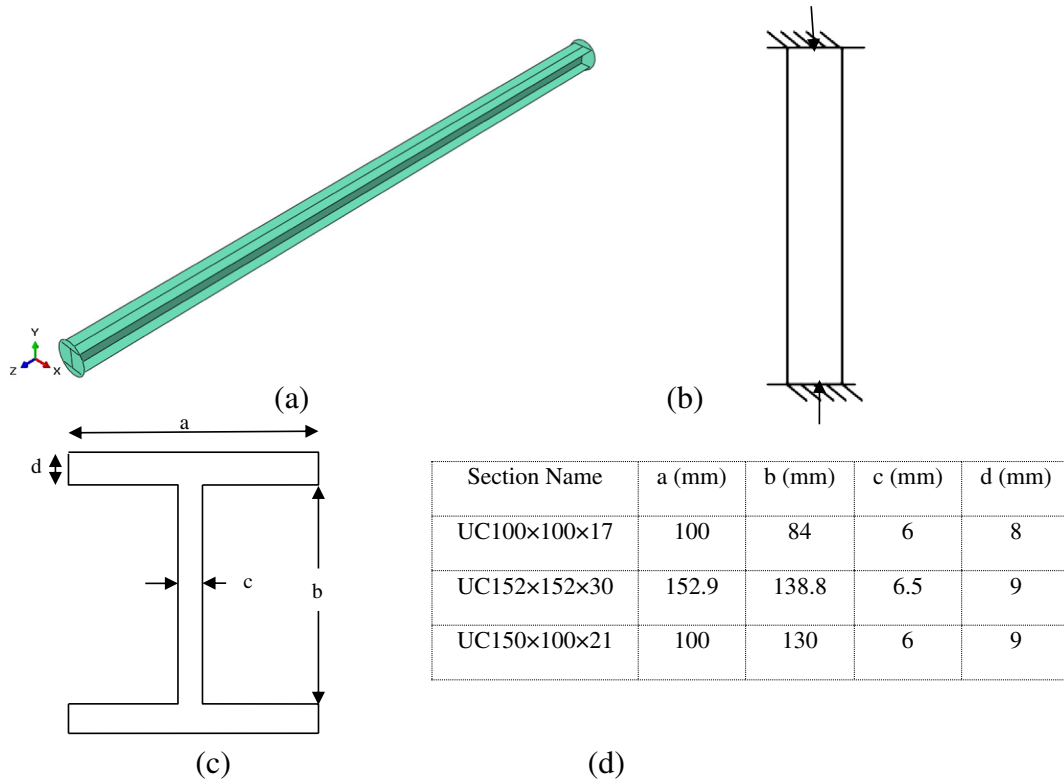


Fig. 1. Geometric description of the UC sections used in the current study; (a) FE model, (b) fixed-fixed column, (c) cross-section, and (d) dimensions used in FE analysis.

iterative approach were the calculated buckling loads, coefficients of the various mode shapes involved and analytical forms of the failure mode shapes anticipated. Serra [13] used Fourier series to analytically prove that inducing a rotation angle to the geometry of a column positively

impacts its critical buckling load. Recently, Sahu and Asha [10] studied the stability analysis of ply-laminated composite pretwisted panels using finite element analysis with 8-node quadratic shell elements. Specifically, they have studied the effect of different parameters such as

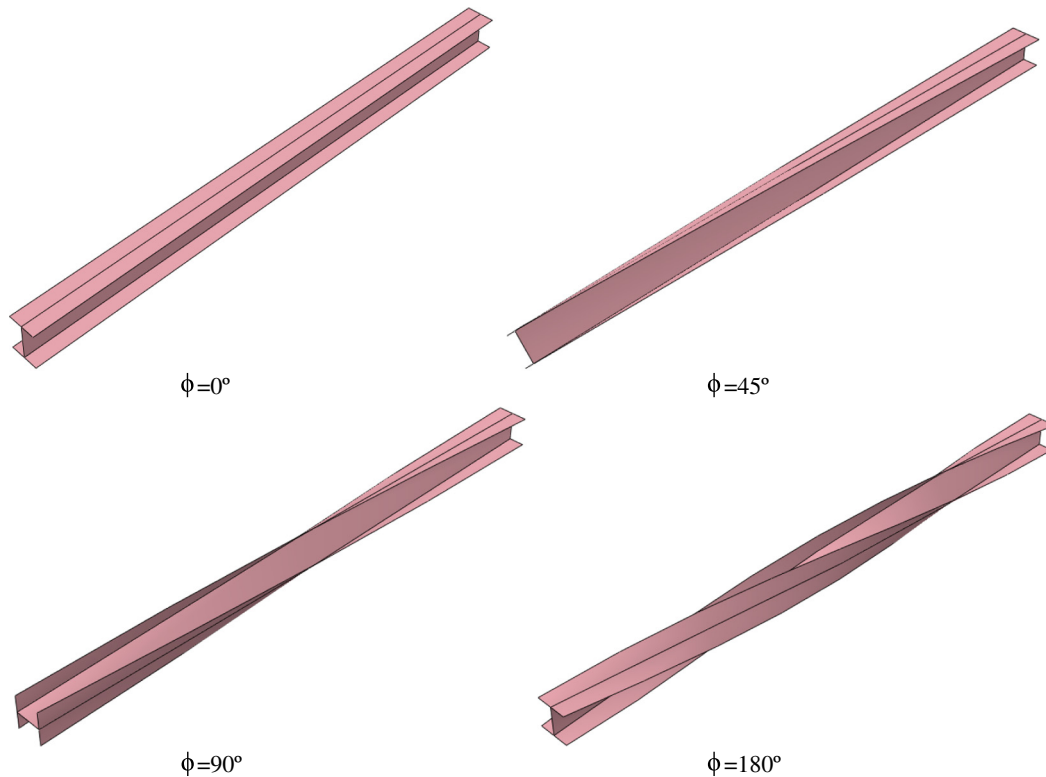


Fig. 2. Samples of pretwisted geometries for UC100 × 100 × 17 columns at selected angles.

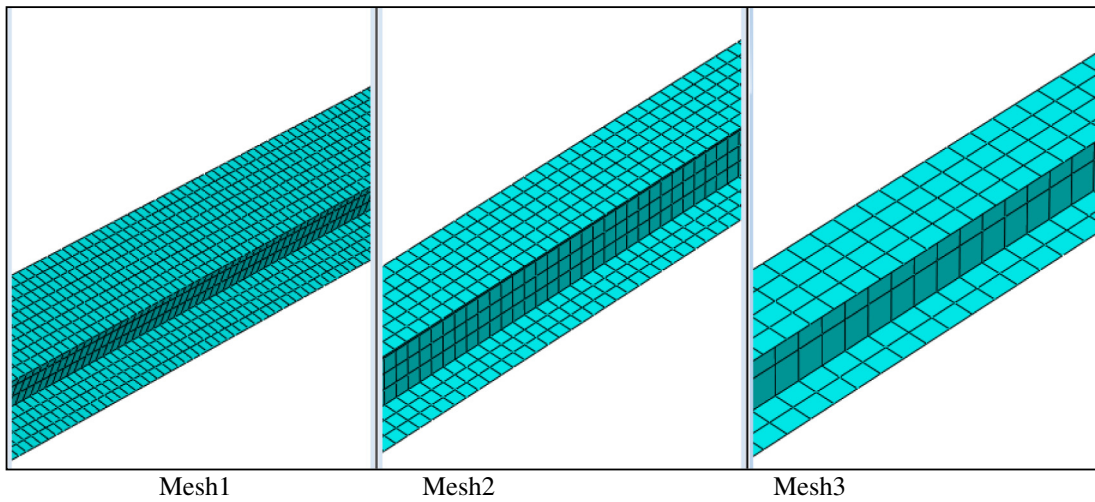


Fig. 3. Three different mesh configurations used in the mesh sensitivity analysis.

angle of pretwist, aspect ratio, lamination parameters, and shallowness ratio on the vibration and stability of pretwisted panels. Several other studies have been also conducted with different applications of pretwisting effect (e.g., [4,5,7,8,11,17]).

Most recently, Barakat and Abed [2] conducted an experimental study to investigate the effect of pretwisting on the axial load capacity and stability of fixed-ended pretwisted steel bars with rectangular cross-sections. More than 200 specimens of different cross-sections, lengths, and widths were first twisted with several angles using a torque machine, and then compressed using MTS machine. The experimental study was then expanded by using non-linear finite element analysis to include a wider range of pretwisting angles up to 270° [1]. Both the experimental and numerical results concluded that pretwisting increases the buckling capacity of thin columns; the buckling load capacity becomes higher with higher ratios of principle moments of inertia for a specific set of pretwisting angles. It was also observed that the buckling load of a pretwisted bar is always higher than that of the corresponding prismatic bars with unequal principal moments of inertia. Also, the highest increase in buckling capacity of the bars was observed at a pretwisting angle close to 90°.

Pretwisting was widely used with beams in helicopter rotor blades, turbine blades and gear teeth [9]. The aim of this research is to extend its application in steel construction, particularly in bracing members with proper encasements. The present research will be directed to study the effect of pretwisting on the buckling strength of universal steel columns. Elastic buckling analysis will be performed using linear perturbation approach that is implemented in the commercial finite element code ABAQUS [6]. The proposed analysis includes buckling performance of fixed- and pinned-ended UC sections that are initially pretwisted at several angles of twists.

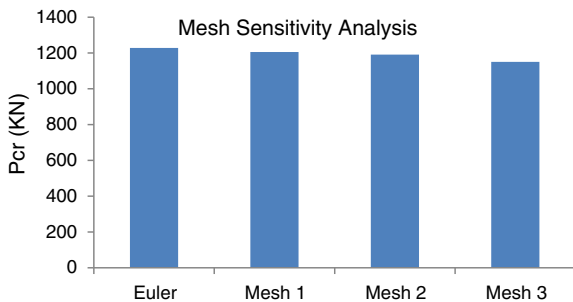


Fig. 4. Bar chart comparisons of the critical loads between FE analysis and Euler equation using three different mesh configurations.

2. Linear perturbation analysis

In this research, buckling of pretwisted columns is solved numerically using linear perturbation analysis technique that is available in the finite element software ABAQUS. The linear perturbation analysis step is created such that the response can only be linear, estimating elastic buckling by the use of Eigen value extraction. Eigen value buckling analysis is utilized in the linear perturbation analysis step to analyze preloaded or unloaded stiff structures. This type of analysis step is, therefore, considered suitable for the focus of the present research dealing with elastic (Euler) buckling of stiff and unloaded compression members.

The Euler column, responds very stiffly to the applied compressive load, until the critical buckling load is reached. A sudden failure of the column, referred to as Buckling, is then observed, and the column shows a much lower stiffness value. The buckling load is usually calculated on the base state of a column. Thus, estimation using general Eigen value extraction is useful since the perturbation load is elastic before the buckling occurs. The key point in an Eigen value problem is

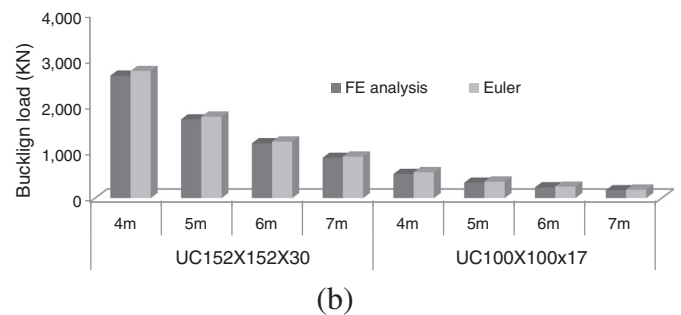
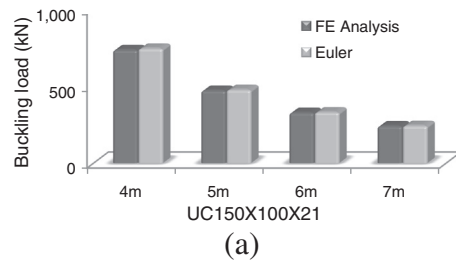


Fig. 5. FE model verifications for different column lengths; (a) non-boxed, and (b) boxed sections.

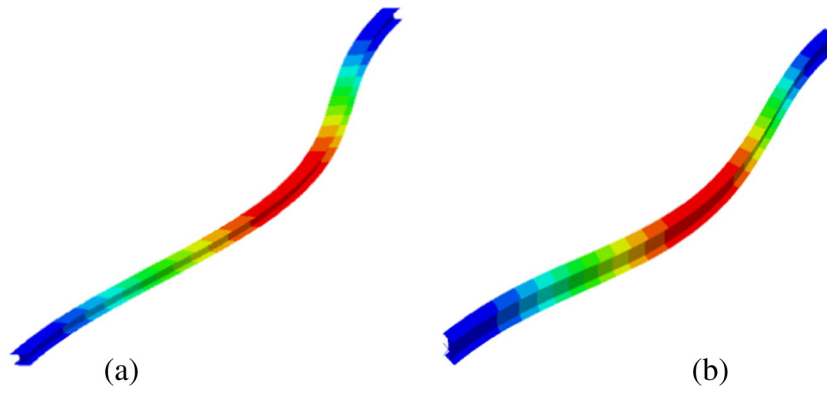


Fig. 6. Flexural buckling modes for selected untwisted UC columns ($\phi = 0^\circ$), (a) UC100X100X17 with $L = 5$ m and (b) UC150X100X21 at $L = 4$ m.

making the model stiffness matrix singular, such that the problem is described by the following relation [6]:

$$K^{MN} u^M = 0 \tag{1}$$

where K^{NM} is the tangent stiffness matrix and u^M is the displacement vector. In this buckling analysis step an incremental load pattern, whose magnitude is not of great importance, will be scaled by the load multipliers λ_i such that the Eigen value problem can be defined by a much general equation:

$$(K_o^{MN} + \lambda_i K_\Delta^{MN}) u_i^M = 0 \tag{2}$$

where K_Δ^{NM} is related to the differential loading pattern while K_o^{NM} corresponds to the initial loading condition. The superscripts M and N are the degrees of freedom for the whole system while the subscript i denotes the i th buckling mode. Here, $K_o^{NM} = 0$ since the UC sections used in this study are not preloaded. In Eq. 2 λ_i are the Eigen values and the vectors u_i^M are normalized so that the maximum displacement is equal to 1.0 which represents the different buckling modes, and not the actual deformation values at the critical buckling load. The subspace iteration Eigen solver is used in this analysis step, based on the number of Eigen values specified. However, the critical buckling load is taken as the load that corresponds to the first buckling mode for each twisting angle.

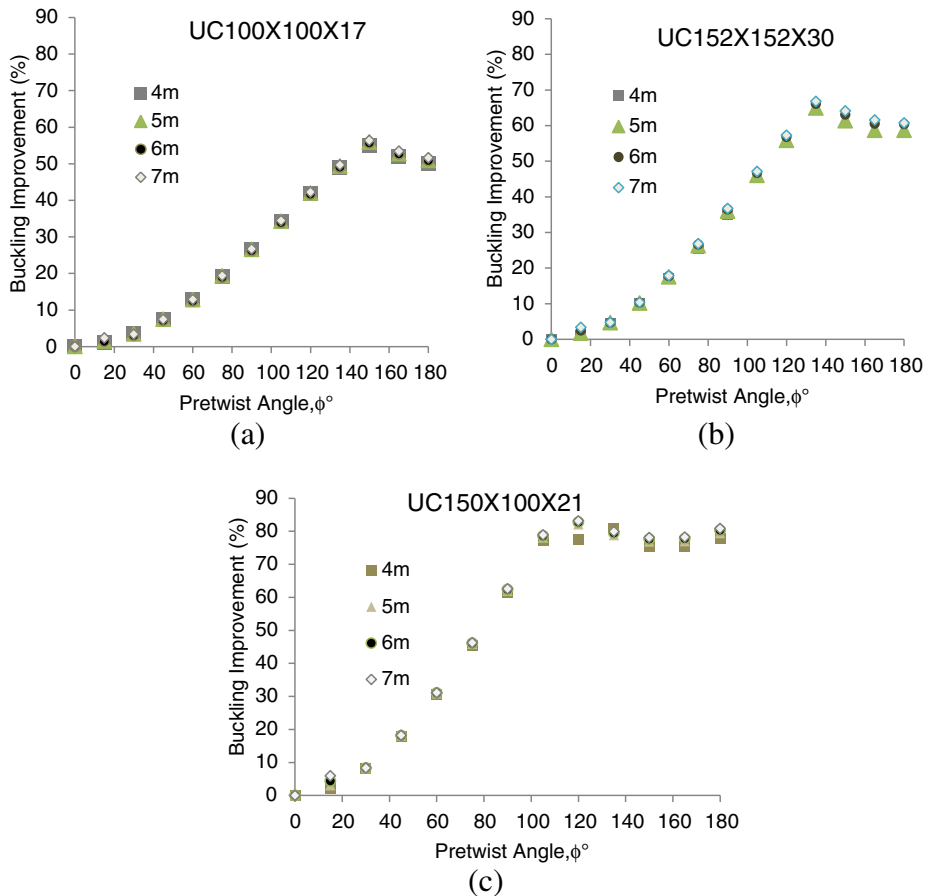


Fig. 7. Buckling improvement versus angle of twist for boxed (a & b) and non-boxed (c) sections.

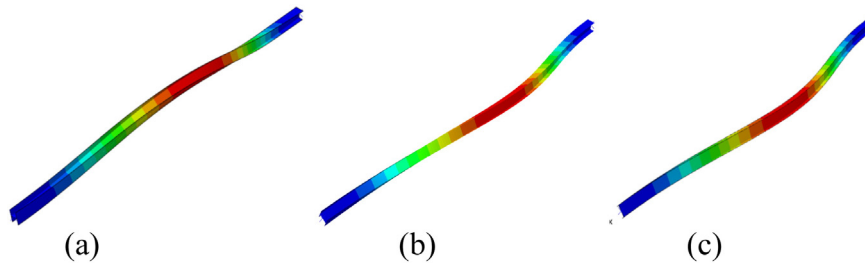


Fig. 8. Samples of buckling modes for the boxed sections (a) $L = 4$ m, $\phi = 105^\circ$, (b) $L = 6$ m, $\phi = 165^\circ$, and the non-boxed section (c) $L = 5$ m, $\phi = 45^\circ$.

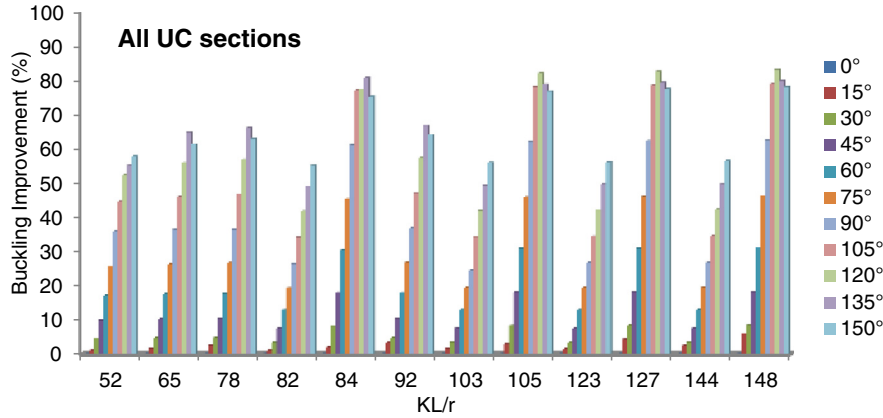


Fig. 9. Histograms of Buckling improvement versus slenderness ratio up to $\phi = 150^\circ$.

3. FE modeling using linear perturbation

Finite element (FE) modeling of pretwisted columns was developed using the commercial software ABAQUS 6.10. The FE simulations were performed using the (*BUCKLE) procedure that is available in the ABAQUS library which adopts the Eigen value analysis procedure described in the previous section. The aim of the FE analysis was to investigate the improvement of the axial capacity in pretwisted wide-flanged steel columns. Only the first (critical) buckling mode predicted from the Eigen value analysis was considered. Three different Universal Columns (UC) sections with different lengths were investigated in this study; UC100 × 100 × 17, UC152 × 152 × 30, and UC150 × 100 × 21. Fig. 1 shows a detailed description of the sections used in this FE analysis. As can be noticed, only UC150 × 100 × 21 among the three columns has a cross-section with unequal depth and width, i.e. not a boxed section.

Each column was modeled using a three-dimensional (3D) shell part and meshed with 4-node 3D shell elements of S4R type. The general-purpose shell element S4R provides robust and accurate solution in various loading conditions for thin and thick shell problems. It is formulated such that thickness change as a function of in-plane deformation is allowed. In the present analysis, Simpson integration rule was adopted with five integration points along the thickness of the webs and flanges of the straight and pretwisted columns. Two analytical rigid plates were created and attached to the original column. A reference point was introduced for each rigid plate to identify the boundary conditions on each end. A fixed–fixed end condition was introduced such that the rotation and translations are restricted at the supports. One support end, however, was allowed to translate in the direction at which the unit load is applied.

Different rotational angles and column lengths have been considered in the present FE analysis. Since most of the columns used in

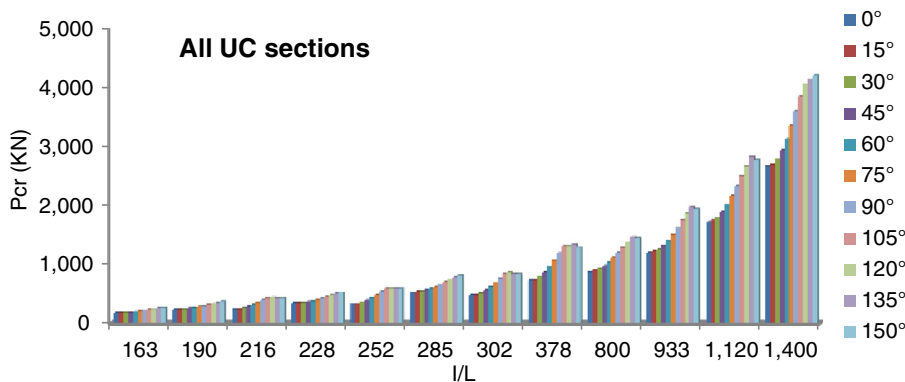


Fig. 10. Histograms of critical loads versus I/L ratio (the ratio of the weak moment of inertia to the specimen length) up to $\phi = 150^\circ$.

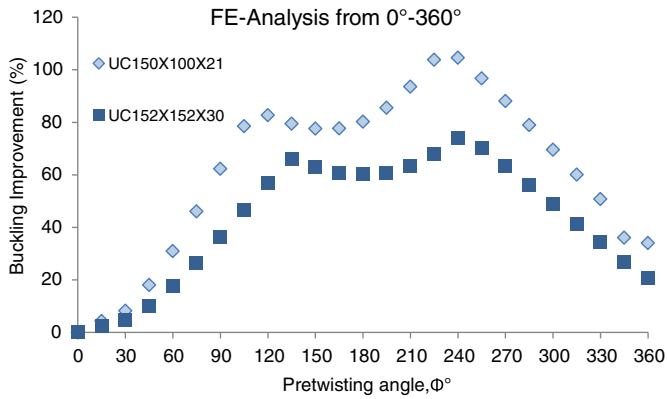


Fig. 11. Increase in buckling capacity at pretwisting angles, ϕ up to 360° for boxed and non-boxed sections.

steel structures have a height of more than 3.0 m, the minimum considered column length in this study was 4.0 m and an increment of 1.0 m was then taken till a maximum column height of 7.0 m. For each column length, a set of pretwisted angles between 0° and 180° with an increment of 15° were considered. Fig. 2 shows examples of the overall geometry of a pretwisted column at selected rotations. Eigen value analysis was then performed to obtain the buckling capacity and the failure mode for each column. This is done by applying a unit load at one end of the rigid support. From this particular analysis, buckling modes and critical loads were obtained and the expected improvement in the column axial capacity was recorded.

3.1. Mesh sensitivity analysis

To decide on the appropriate mesh that gives the most accurate results while minimizing the needed computational time, different mesh configurations should be examined. Mesh sensitivity analysis was, therefore, conducted in this study by considering three mesh configurations as shown in Fig. 3; Mesh1, Mesh2 and Mesh3 with global element sizes of 20 mm, 25 mm and 50 mm, respectively. The three meshes were used to simulate the buckling capacity of untwisted and twisted UC152 × 152 × 30 column of 6 m length. Mesh1 and Mesh2 were found to give similar accuracy when compared with the calculated values using Euler Equation as illustrated by the bar chart shown in Fig. 4. The total difference between the results given by Linear Perturbation Analysis using Mesh1 or Mesh2 was less than 3%, whereas, it exceeds 6% when using Mesh3. Therefore, Mesh2 was selected in the present FE analysis since it gives an acceptable combination of accuracy and reduced computational time.

3.2. FE model verification

The elastic buckling load for straight columns (i.e., at an initial pretwisting angle of 0°) was obtained analytically using the well-known Euler equation given below:

$$P_o = \frac{n^2 EI}{(KL)^2} \tag{3}$$

where P_o denotes the critical buckling capacity corresponds to the first buckling mode, E is the modulus of elasticity (200 GPa), I is the moment of inertia of the cross-section about the weak axis, K is the theoretical effective length factor, and L is the column length. Results obtained from the FE buckling analysis for untwisted columns were compared with the analytical solution obtained via Euler equation for each member. The main aim of this comparison was to validate the accuracy of the finite element model. Fig. 5(a) presents the comparison results for the case of the non-boxed section whereas Fig. 5(b) shows the results for the two boxed sections. It can be noticed that good correlations have been achieved by the FE modeling for the three sections and for several length increments. In these comparisons, the length increments were selected such that columns were slender enough to ensure elastic buckling. Fig. 6 shows samples of the expected flexural buckling modes for the fixed-ended untwisted columns. Flexural-torsional buckling was not experienced because the members were not yet pretwisted in the simulation below.

4. Results and discussions

4.1. Improvement of buckling capacity

Utilizing the linear perturbation analysis through the FE simulations of pretwisted columns, critical buckling loads were recorded to study the improvement in buckling capacity due to pretwisting. Fig. 7 shows the percentage increase in the buckling capacity for the three UC sections with respect to the critical loads at $\phi = 0^\circ$ (P_o). Assessment of the FE results for pretwisting up to $\phi = 180^\circ$ indicates that the buckling capacity is always higher than P_o . The percentage increase in the critical loads is therefore always rising, until the optimum pretwisting angle is reached, after which the improvement decreases relatively, but the critical buckling load remains of larger value than the reference P_o .

The increase in the buckling capacity was higher for the case of the non-boxed section (about 85%) as compared with the two boxed sections (between 55% and 65%). On the other hand, the optimum rotational angle, at which the buckling improvement is the maximum, took a different trend. For UC100X100X17, the optimum angle was around 120° , while for the other boxed section UC152X152X30, it was 150° . For the non-boxed section, however, the maximum improvement was achieved at $\phi = 120^\circ$, similar to the smaller boxed section. Further twisting seems to give less axial capacity for all sections as shown in

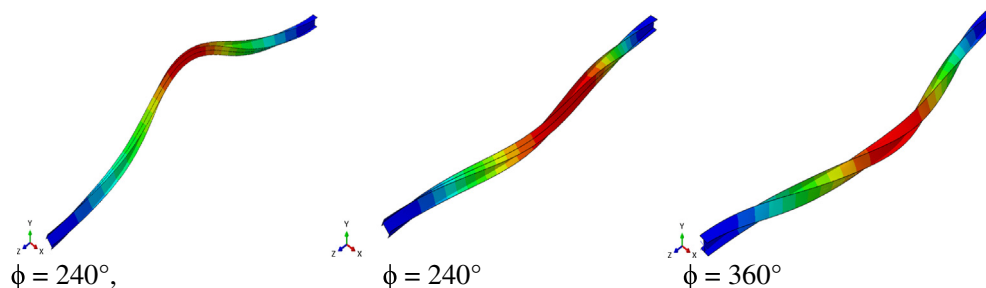


Fig. 12. Buckling modes for selected sections at high pretwisting angles.

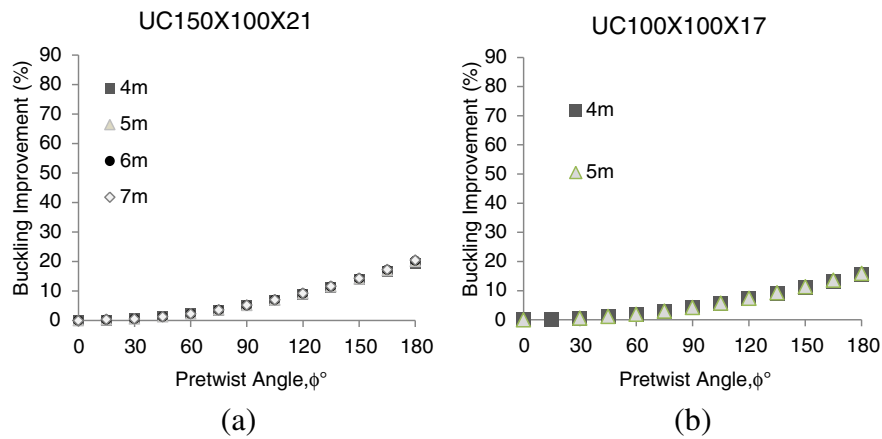


Fig. 13. Increase in buckling capacity with pretwisting for pinned-pinned columns for (a) non-boxed and (b) boxed sections.

Fig. 7. It can also be noticed from Fig. 7 that the percentage and rate of increase in the buckling capacity for a column remain more or less the same with any given length. This could be observed for all UC sections. Thus, the original length of the member would not be correlated with the pretwisting angle, ϕ in justifying the buckling improvement. Consequently, it can be concluded that the variation in the section's moment of inertia about the two axes with ϕ controls the increase in buckling capacity of the pretwisted member, for a given boundary condition (i.e., K is constant).

4.2. Failure modes

The proposed FE model was capable of accurately predicting the failure modes of the pretwisted members, mainly flexural and flexural-torsional buckling. Although, flexural buckling controlled the results of most simulations, flexural-torsional buckling took place for a number of pretwisted columns. For the case of the boxed sections, flexural-torsional buckling modes were attained as a result of the permanent twist for a range of angles between 105°–150°. On the other hand, the main failure mode for the non-boxed section was flexural buckling, and no torsional failure modes were observed for the lengths and angles considered.

During buckling, the pretwisted steel sections assumed non-planar deformed configurations, and remained in the elastic zone so they failed due to buckling and not yielding. The compression members were slender enough to claim global buckling as shown in the deformed shapes presented in Fig. 8.

4.3. Discussions

As per the definition of global buckling, compression member is expected to go through extensive lateral translation in the weak-direction. As the pretwisting is applied, the weak and strong directions exchange roles along the length of the compression members. In other words, the weak direction is strengthened and the strong direction is getting weaker. This transition between the strong and weak axes, leads to the overall increase in buckling capacity of the pretwisted member. As the angle of the twist is increasing, one can no longer predict the direction about which failure would take place. However, about whichever direction buckling occurs, it will always be at a greater critical load than that for a non-pretwisted member.

For all UC sections considered in this study, elastic buckling results predicted using linear perturbation analysis showed a sharp increase in buckling capacity up to 65–90% improvement as compared with non-twisted sections. The pretwisting angles, at which the critical buckling load is maximum, ranging between 120° and 150°. This is clearly perceived in the histograms shown in Figs. 9 and 10. It is quite apparent that with higher slenderness ratios, the improvement in axial load capacity reaches its maximum at smaller pretwisting angles than for the case of lower slenderness ratios. Furthermore, the percentage of increase in the buckling capacity of members with higher slenderness ratios is much higher than that of sections with lower slenderness ratios. For example, maximum enhancement in the axial load capacity was reached at $\phi = 150^\circ$ for the lower slenderness ratio of $KL/r = 52$, while for the highest slenderness ratio ($KL/r = 148$), the maximum improvement was achieved at $\phi = 120^\circ$, as illustrated in Fig. 9. Similarly, a

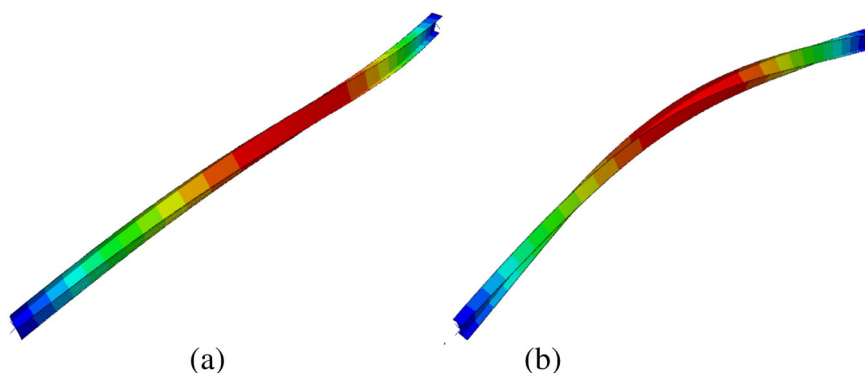


Fig. 14. Buckling modes of pin-ended columns (a) non-boxed, $\phi = 90^\circ$, (b) boxed, $\phi = 180^\circ$.

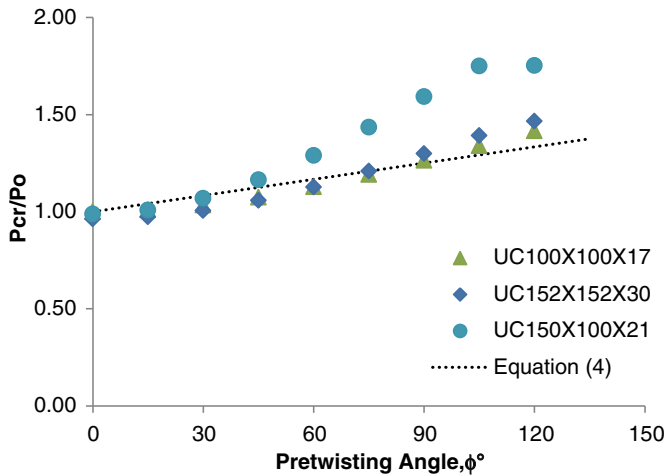


Fig. 15. Comparison of FE analysis against proposed Eq. 4.

sharp increase in the critical load up to $\phi = 120^\circ$ – 150° is also noticed (see Fig. 10) at larger ratios of I/L , where I denotes the cross sectional moment of inertia about the weak axis and L is the length of the specimen.

4.4. Linear perturbation analysis for ϕ up to 360°

For further investigation on the effect of pretwisting on the column's axial capacity, the range of pretwisting angles chosen for analysis was extended up to $\phi = 360^\circ$. Accordingly, buckling analysis was conducted at pretwisting increments of 15° each on boxed and non-boxed sections for a fixed length of 6 m as shown in Fig. 11. As explained earlier, the buckling improvement for the non-boxed section keeps increasing until it reaches a maximum of 83% at $\phi = 120^\circ$, then slightly decreases between 120° and 165° . The buckling capacity starts increasing again up to 100% at $\phi = 240^\circ$, after which it keeps decreasing sharply as the pretwisting angles reach 360° . A similar trend was noticed for the case of the boxed section, but with less percentage of improvement at a higher pretwisting angle $\phi = 135^\circ$. However, the rotation angle $\phi = 240^\circ$ remains the optimum for FE analysis beyond $\phi = 180^\circ$ for both sections (see Fig. 11). Samples of buckling modes for the case of large pretwisting angles are also presented in Fig. 12.

4.5. Buckling improvement under pinned–pinned conditions

Elastic buckling analysis on pretwisted columns with pinned–pinned end condition was also investigated to study the effect of the end conditions on the improvement in buckling capacity. The members picked for this investigation were UC100X100X17 and UC150X100X21. Pinned end condition was introduced such that in-plane translations are restricted at the supports and the rotation was allowed around the weak axis. Applying pinned–pinned boundary conditions however, proved a relatively negligible improvement as compared with the fixed–fixed boundary condition. The improvement witnessed in the non-boxed section was slightly higher than that recorded for the boxed section, as can be seen from Fig. 13. The increase in the buckling capacity, however, could not exceed 20% for either section. This low improvement may be attributed to the fact that under pinned–pinned condition the rotation is not restricted at the two ends. The member is free to rotate starting at the two supports, where the least effect of pretwisting is noted. On the other hand, under fixed–ended condition, rotation of the member is restricted to only 0.5–0.65 of the whole length, mostly acting in the region where pretwisting is most effective. Samples of buckling modes for selected pin-ended sections are presented in Fig. 14.

5. Mathematical model to compute critical buckling load

As mentioned earlier, [2] and Abed et al. [1] performed experimental and numerical investigations on buckling improvement for a set of steel bars with varying thicknesses, widths and lengths, and for pretwisting angles up to 270° . The maximum buckling improvements for the sections considered were achieved at optimum pretwisting angles between 75° and 90° . Consequently, Abed et al. [1] used Multiple Regression Analysis to propose two definitions that relate the critical loads to pretwisting angles for the case of elastic and inelastic buckling. To serve the purpose of the current study, the equation for elastic buckling given in Eq. 4 was utilized for comparisons with the linear perturbation analysis performed in this study.

$$P_{cr}^{\text{pretwisted}} = \left[1 + \frac{\phi}{360} \right]^n P_o. \quad (4)$$

The power constant n is set to a value of 1.0 to give conservative predictions of the buckling capacity at different angles of twist. The main aim behind Eq. 4, was to be able to predict the axial buckling capacity of a pretwisted ($\phi \leq 90^\circ$) compression member, regardless of its slenderness ratio, section properties or length. Fig. 15 shows a comparison between the buckling improvements predicted by Eq. 4 and the present analysis for the three considered sections at a fixed length of 4 m. By taking a closer look at the plotted graph, one can thus conclude that the proposed equation can be generalized to be used for the present compression members. The proposed Eq. 4 predicted conservative critical loads as compared with the results obtained by the present FE analysis for all sections considered. It should be emphasized that the applicability of Eq. 4 is limited to fixed–ended pretwisted steel columns with rotation angles not to exceed 90° .

6. Conclusions

Elastic buckling of pretwisted fixed–ended steel columns was studied using linear perturbation analysis through finite element modeling. Universal columns with three different cross-sections of various lengths, initially twisted at angles from 0° – 180° , were analyzed in this study. The expected effect of pretwisting was to improve the buckling capacity of the compression members. Consequently, permanent pretwisting is to be perceived as an effective technique to increase the strength of any steel compression member. Results showed that there is a significant improvement in the critical buckling capacity for different slenderness ratios. A sharp increase in buckling capacity up to 90% improvement as compared with non-twisted sections was demonstrated in most sections. However, the effect of various column lengths on the buckling improvement for a given UC section was insignificant. The present FE analysis was examined by comparison with the results predicted by the earlier proposed equation by Abed et al. [1] and good agreement was achieved.

Buckling capacity of pretwisted UC sections with pinned–pinned end conditions was also investigated. The improvement in the axial capacity was found to be very small as compared with its fixed–ended counterparts. Only 20% maximum increase in the buckling capacity was achieved for the three UC sections used in this study.

References

- [1] Abed F, AlHamaydeh M, Barakat S. Nonlinear finite element analysis of buckling capacity of pretwisted steel bars. *J Eng Mech* 2013;139:791–801.
- [2] Barakat S, Abed F. Experimental investigation of the axial capacity of inelastically pretwisted steel bars. *J Eng Mech* 2010;136:1028–35.
- [3] Celep Z. Stability of pretwisted Leipholz' column. *Acta Mech* 1986;60:157–70.
- [4] Chen CH, Yao Y, Huang Y. Elastic flexural and torsional buckling behavior of pretwisted bar under axial load. *Struct Engn Mech, An Int'l Journal* 2014;49:273–83.
- [5] Chen WR. Dynamic stability of linear parametrically excited twisted Timoshenko beams under periodic axial loads. *Acta Mech* 2011;216:207–23.
- [6] Hibbitt, Karlsson, Sorensen. Inc. ABAQUS standard 6.12, USA; 2012.

- [7] Kim S, Lee K. Potentials of elastic seismic design of twisted high-rise steel diagrid frames. *Steel & Composite Struct, An Int'l Journal* 2015;18:121–34.
- [8] Leung AY. Dynamic buckling of thin pre-twisted beams under axial load and torque. *Int J Struct Stab Dyn* 2010;10:957–63.
- [9] Lin S, Wong W, Lee S. The dynamic analysis of nonuniformly pretwisted Timoshenko beams with elastic boundary conditions. *Int J Mech Sci* 2001;23:85–2045.
- [10] Sahu S, Asha A. Stability of laminated composite pretwisted cantilever panels. *J Reinf Plast Compos* 2005;24:1327–34.
- [11] Sakar G, Sabuncu M. Dynamic stability analysis of pretwisted aerofoil cross-section blade packets under rotating conditions. *Int J Mech Sci* 2008;1–13.
- [12] Segui WT. *Steel Design*. 4th edition. Stamford: Cengage Learning; 2007.
- [13] Serra M. Flexural buckling of pretwisted columns. *J Eng Mech* 1993;119:1286–92.
- [14] Steinman DA, Tabarrok B, Cleghorn WL. The effect of pretwisting on the buckling behaviour of slender columns. *Int J Mech Sci* 1991;33:249–62.
- [15] Tabarrok B, Xiong Y, Steinman D, Cleghorn WL. On buckling of pretwisted columns. *Int J Solids Struct* 1990;26:59–72.
- [16] Yang YB, Yau JD. Stability of pretwisted bars with various end torques. *J Eng Mech* 1989;115:671–88.
- [17] Zhao Z, Zhao H, Chang Z, Feng X. Analysis of bending and buckling of pre-twisted beams: a bioinspired study. *Acta Mech Sinica* 2014;30:507–15.